Abbas Dashtimanesh
Parviz Ghadimi

ISSN 0007-215X
eISSN 1845-5859

SPS TURBULENT MODELING OF HIGH SPEED TRANSOM STERN FLOW

UDC 629.5.015.2
Original scientific paper

Summary

Transom stern flow is a complicated fluid flow phenomenon especially at high speed regime. Therefore, various authors have studied the transom stern flow, both numerically and experimentally. Smoothed Particle Hydrodynamics method can be considered as a good choice for simulation of nonlinear physics related to the transom flow. Accordingly, SPH as a meshless, Lagrangian, and particle method is presented in this article and SPS turbulent model is also included for more accurate solution. For density modification, a second order density filter scheme is employed. For validation of numerical setup, several draft based Froude numbers are considered and it is shown that SPH solution is in good agreement with available experimental data. Furthermore, three longitudinal Froude number are investigated for high speed transom flow simulation. High speed cases are compared with Savitsky's formula and it is observed that at high speeds, SPH solutions are also reasonable.

Key words: *SPS Turbulent Model, Transom Stern, High Froude Numbers, Rooster Tail*

Nomenclature

ρ :	Density
p :	Pressure
ν :	Kinematic viscosity
g :	Gravity acceleration
L :	Ship length
u :	Fluid velocity
r :	Vector position (distance between two points i and j)
h:	Smoothing length
q :	r/h
W:	Kernel function
m_j :	Mass of particle j
ρ_j :	Density of particle j
t :	Time

T_T : Transom Draft
n : Number of time step
γ : Polytrophic constant
λ_w : Wave length
B : Constant related to the bulk modulus of elasticity of the fluid
T : SPS stress tensor
S : Wave slope
Fr_T : Draft based Froude number
Fr_L : Longitudinal Froude number
$\beta(r_i)$: Correction vector

1. Introduction

Transom stern has been widely used in last decades and from very beginning of planing crafts design, it was used to obtain the separation of flow. It may be due to this fact that transom stern resistance is less than the equivalent streamline form, based on experiments of Maki [1] on a backward facing step with free surface (BFSFS). BFSFS is an infinite-beam rectangular section with an abrupt change in its height which has been considered as a simplified transom stern geometry by some authors. Furthermore, simulation of transom wave, especially at high Froude numbers, has also been one of the main computational challenges for many of researchers.

In this context, some researchers have studied to study high speed transom flow, experimentally. Doctors [2] studied the ventilation process at transom stern of a high speed craft. An extensive set of experiments were conducted on five parent hulls for simple rectangular section ship models. Finally, a regression formula was derived and it was found that height of transom wave is a function of draft based Froude number

$$Fr_T = U / \sqrt{gT_T}$$

Where U is hull speed, g is gravity acceleration and T_T is draft at transom location. Doctors [3] further analyzed the previous experimental findings and derived a regression formula for estimation of the transom ventilation. Two series of experiments were also conducted by Maki et al [4]. They studied transom flow for two different high speed destroyers. Transom wave was measured and an empirical relation for transom drying was extended.

In all of the above studies, considered Froude numbers were lower than the planing condition. Savitsky [5] used experimental data and reformulated the problem by suggesting a relation which was a function of various parameters. More recently, Savitsky and Morabito [6] performed an extensive set of experiment on the transom flow of a planing hull, for the first time and derived a set of formulas for estimating free surface profile, just behind the transom stern.

Moreover, some authors implemented various numerical methods for high speed transom stern flow simulation in order to avoid very expensive experiments. In this context, viscous numerical solution of high speed transom flow was presented by Haussling et al. [7]. Maki et al. [8] also performed a detailed numerical study using level set method to simulate various physical features of transom flow problem. They compared the obtained results with experiments of Maki [1]. Some inconsistencies between experimental and numerical results were observed and they found that these discrepancies were due to inaccurate turbulent

modeling. Although, Marrone et al. [9] presented a smoothed particle hydrodynamics (SPH) solution to study the breaking wave pattern generated by a fast ship, there exists a need for applying SPH in marine hydrodynamic applications. One may legitimately claim that SPH has been used less in the field of naval architect than other numerical methods.

Therefore, based on our knowledge from the presented literature survey, employing turbulent SPH method for transom flow computation can be considered as a novelty in marine hydrodynamics. In addition to SPH application in marine hydrodynamic field, transom wave simulation in the case of semi-displacement as well as planing regime is also another important feature of the current study. Therefore, the main aim of the present article is presenting sub particle scale (SPS) turbulence model in conjunction with SPH method for high speed transom flow simulation.

Generally, smoothed particle hydrodynamics is a free mesh Lagrangian method which was separately initiated by Lucy [10] and Gingold and Monaghan [11] in astrophysical phenomena. Although, the SPH method had been used in astrophysical phenomena, Monaghan [12] noticed that the governing equation of astrophysical problems are similar to that of fluid flows equations. Therefore, he developed the SPH formulation for the free surface computations. After that, several authors have implemented SPH to study the fluid flow phenomena in various fields of marine engineering. For an extensive review of recent progress and developments in the SPH, readers are referred to papers by Monaghan [13], Cleary et al. [14] and Liu and Liu [15].

In the current work, transom stern flow is considered as a complicated fluid flow phenomenon in the marine hydrodynamics. Simulations are performed using smoothed particle hydrodynamics. For more accurate simulations, a sub particle scale (SPS) turbulent model is also investigated. Furthermore, to remove numerical instabilities in free surface computations, a second order density filter is also implemented. Transom flow, at various high Froude numbers (draft based) as well as three longitudinal Froude numbers, are conducted. It must be noted the term longitudinal Froude number (Fr_L) denotes on Froude number based on the hull length.

2. Governing equations

The basic governing equations of free surface flows are based on the Lagrangian form of continuity and momentum Navier-Stokes equations:

$$\frac{d\rho}{dt} = -\rho \nabla . \vec{u} \tag{1}$$

$$\frac{d\vec{u}}{dt} = -\frac{1}{\rho}\nabla . p + \nu \nabla^2 \vec{u} + \vec{g} \tag{2}$$

where ρ is the density, p is the pressure, ν is the kinematic viscosity and g is the gravity acceleration. The SPH equations of motion are derived based on these governing equations in Lagrangian form.

3. SPH formulation

3.1 SPH basics

SPH method is fundamentally based on integral interpolants. Therefore, any function $A(r)$ can be approximated by (kernel approximation):

$$A(r)=\int_{\Omega}A(r^{'})W(r-r^{'},h)dr^{'} \tag{3}$$

where r is the vector position and the influence domain is controlled by the value of smoothing length h. $r^{'}$ is also vector position of particles inside smoothing length. By discretization of the approximation (Eq. 3), the particle approximation of the function at a particle, i, can be written as follows:

$$A(r)=\sum_{j}m_{j}\frac{A_{j}}{\rho_{j}}W_{ij} \tag{4}$$

where all the particles within the region of compact support of the kernel function must be considered at the summation. $W_{ij}=W(r_{i}-r_{j},h)$ is the weight function or kernel and m_{j} and ρ_{j} denote the mass and density, respectively. Moreover, the kernel function must satisfy some conditions such as [16]:

1. Positivity $W(r-r^{'},h)\geq 0$ inside the domain Ω
2. Compact support: $W(r-r^{'},h)=0$ out of the domain Ω
3. Normalization: $\int_{\Omega}W(r-r^{'},h)dr^{'}=1$
4. Delta function behavior: $\lim_{h\to 0}W(r-r^{'},h)dr^{'}=\delta(r-r^{'})$
5. Monotonically decreasing behavior of $W(r-r^{'},h)$

The kernel function used in this work is the one originally introduced by Monaghan and Lattanzio [17]:

$$W(r,h)=\alpha_{D}\begin{cases}\frac{3}{4}q^{3}-\frac{3}{2}q^{2}+1 & 0\leq q\leq 1\\ \frac{1}{4}(2-q)^{3} & 1\leq q\leq 2\\ 0 & q\geq 2\end{cases} \tag{5}$$

where α_{D} is $10/(7\pi h^{2})$ in 2D and $q=r/h$. r is the distance between two points i and j.

3.2 SPH implementation

SPH equation can be implemented on any arbitrary function such as density and velocity. Therefore, continuity equation, as one of the governing equations, is discretized based on particle approximation of density for a given particle i as in

$$\frac{d\rho_{i}}{dt}=\sum_{j}m_{j}(u_{i}-u_{j}).\nabla_{i}W_{ij}\ . \tag{6}$$

The discretized momentum equation in SPH formulation can be derived similar to the continuity density approach. The SPH equation of motion, in the absence of dissipation, is therefore given by

$$\frac{du_i}{dt} = -\sum_j m_j \left(\frac{P_i}{\rho_i^2} + \frac{P_j}{\rho_j^2} \right) \nabla_i W_{ij} \tag{7}$$

which can be seen to explicitly conserve momentum, since the contribution of the summation to the momentum of particle *i* is equal and opposite to that given to particle *j*. Furthermore, the equation governing the position of a particle *i* at each time step is

$$\frac{dr_i}{dt} = u_i \,. \tag{8}$$

4. Numerical details

For accurate simulation of high speed transom stern flow, it is imperative to employ some numerical techniques for SPH solution of governing equations. Required schemes are described in the following subsections.

4.1 Time stepping algorithm

Symplectic time stepping algorithm is implemented for time integration of governing equations. Symplectic scheme only has a low memory usage which can be very important issue in SPH method. Based on symplectic method formulation, at step one, density as well as acceleration must be evaluated at the middle of the time step as in

$$\rho_i^{n+1/2} = \rho_i^n + \frac{\Delta t}{2} \frac{d\rho_i^n}{dt}; r_i^{n+1/2} = r_i^n + \frac{\Delta t}{2} \frac{dr_i^n}{dt} \tag{9}$$

where *t* is equal to $n\Delta t$ and n refers to the number of time step. After that, pressure, based on the equation of state, should be calculated. Subsequently, the velocity is obtained from $\frac{d(\omega_i \rho_i v_i)^{n+1/2}}{dt}$ such that position of particles at the end of the time step will be:

$$\begin{aligned} (\omega_i \rho_i v_i)^{n+1} &= (\omega_i \rho_i v_i)^{n+1/2} + \frac{\Delta t}{2} \frac{d(\omega_i \rho_i v_i)^{n+1/2}}{dt} \\ r_i^{n+1} &= r_i^{n+1/2} + \frac{\Delta t}{2} v_i^{n+1} \end{aligned} \,. \tag{10}$$

Finally, $\frac{d\rho_i^{n+1}}{dt}$ can be evaluated using the updated values of v_i^{n+1} and r_i^{n+1}, at the end of the time step.

4.2 Density filter

Density of any particle may be easily evaluated by implementing the following equation:

$$\rho_i = \sum_{j=1}^{N} m_j W_{ij} \,. \tag{11}$$

This relation leads to numerical instabilities in free surface computations [17]. Although, continuity equation can be implemented for finding the particle's densities at any time step, applying this equation may not satisfy the global mass conservation at that step. In order to keep the computation stable, a Moving Least Squares (MLS) technique which was

developed by Colagrossi and Landrini [18] is implemented in the current article. They derived a density filter that can exactly reproduce linear variations in the density field. In first step, density field can be reproduced as follows:

$$\bar{\rho}_i = \sum_j \rho_j W_{ij}^{MLS} \frac{m_j}{\rho_j} = \sum_j m_j W_{ij}^{MLS} \tag{12}$$

Afterwards, modified smoothing function can be evaluated as in

$$W_{ij}^{MLS} = W_{ij}^{MLS}(r_i) = \beta(r_i).(r_i - r_j)W_{ij}, \tag{13}$$

where $\beta(r_i)$ is a correction vector.

4.3 Particle interaction

The linked list algorithm is used when searching for the nearest neighboring particles to a particle *i*. The computational domain is meshed by a grid, with a mesh spacing *kh* matching the dimension of the support domain. It is clear that the particle only interacts with the particles in its own and eight neighboring cells. It is not even necessary to search all eight neighbors as the interaction with four of the cells has already been resolved. This reduces the computational time from N^2 to N log N where N is the number of particles [19]. The linked list works best when the smoothing length is constant.

4.4 Equation of state

According to Batchelor [20], the pressure and density are related by means of Tait's equation of state. It can be seen that a small oscillation in density may result in a large variation of pressure:

$$P = B\left[\left(\frac{\rho}{\rho_0}\right)^{\gamma} - 1\right] \tag{14}$$

where ρ_0 = 1000 kg/m^3, γ is the polytrophic constant, usually between 1 and 7. The parameter B is also a constant related to the bulk modulus of elasticity of the fluid. For imposing the zero pressure at a surface, the -1 (minus one) term in the equation of state is present [19].

4.5 Boundary conditions

Here, Dalrymple dynamic boundary condition [21] is applied. Boundary particles have the same behavior as the fluid particles and follow continuity, momentum and state equations. Contrary to the fluid particles which have displacements, boundary particles displacements are zero. When a particle reaches the boundaries, density of the boundary particle is increased. Therefore, because of pressure term (P/ρ) in momentum equation, the force which acts on the particle fluid increases. When the distance between the boundary particle and the fluid particle decreases, density, pressure and acting force on the fluid particle increases by a repulsive mechanism.

4.6 Turbulent modeling

Sub Particle Scale (SPS) model, based on the Large Eddy Simulation (LES) concept, has been included into the SPH equations by Rogers and Dalrymple [21]. In the SPS formulation, the momentum equation is written as follows:

$$\frac{du_i}{dt} = -\frac{1}{\rho}\nabla P + \mu\nabla^2 u + \frac{1}{\rho}\nabla\bar{\tau} + g \ . \tag{15}$$

The laminar stresses can be modeled easily. A Smagorinsky model is also used for the turbulent eddy viscosity and consequently, the SPS stress can be discretized in a manner analogous to the pressure term and is given by

$$\frac{1}{\rho_i}\nabla\bar{\tau}_i = \sum_{j=1}^{N} m_j \left(\frac{\bar{\tau}_i}{\rho_i^2} + \frac{\bar{\tau}_j}{\rho_j^2}\right)\nabla W_{ij} \tag{16}$$

5. Further details on computational and physical considerations

Before presenting the results of transom flow simulation, it seems necessary to have a brief discussion about some computational and physical characteristics such as number of particles, computational time and dynamic trim. Based on the literature related to SPH, it is clear that as the number of particle increases, accuracy is improved. Accordingly, two different particle sizes are considered in the current work to examine CPU time. Table 1 shows that, an increase in the number of particles, leads to a significant increase in computational time. Generally, due to high computational time, the number of particles is kept fixed in all cases. In addition to computational characteristics, it is necessary to describe the effects of constant dynamic trim on computational results. For this purpose, empirical formulas obtained by various authors are examined and it is found that trim has a small influence on the generated rooster tail. For example, a sample of computations is shown in Fig. 1.

Table 1 Comparison of computational time for three different particle size.

Number of particles:	65000	450000	580000
Computational time:	13.5 h	116 h	168 h

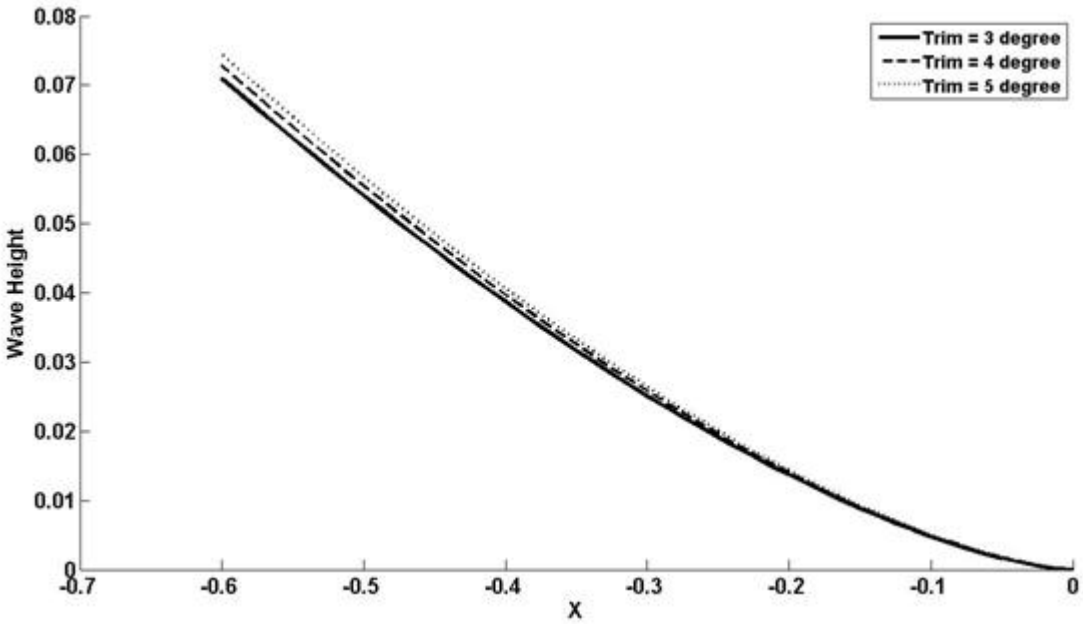

Fig. 1 Effects of trim on generated rooster tail as an example of calculations.

6. Verification of numerical solution

For examining the capability of the presented numerical method for transom flow simulation, a range of draft based Froude numbers is considered, at first. A computational domain which is depicted in Fig. 2 is considered and a simple rectangular body with 1 meter length is moved with a constant velocity. A coordinate system *x*-*z* is also shown in Fig. 2. For validation purposes, both maximum root mean square (*RMS*) (Eq. 17) of the free surface profile and wave slope (i.e. *S = Wave Height / Wave length*) are compared against the experimental [1] as well as numerical solutions [8] existing in the literature. It must be noted that wave slope is representative of both wave amplitude and wave length. Overall, seven draft Froude numbers ranging from 0.5 to 3.5 are investigated in this article.

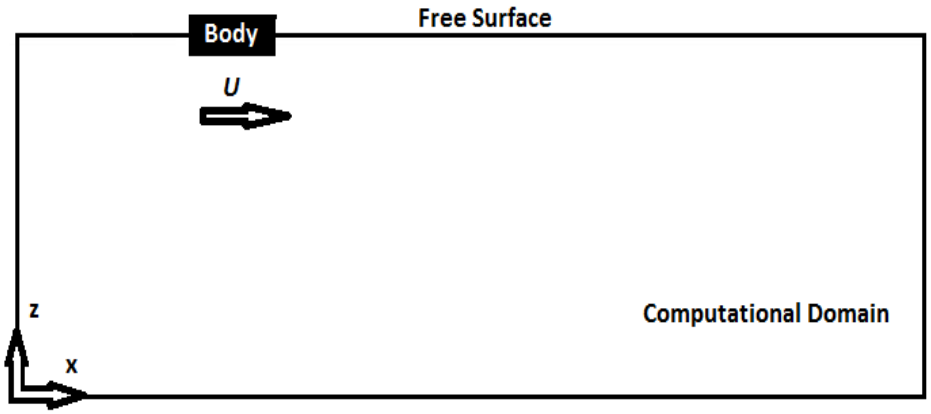

Fig. 2 Computational domain.

Size of the computational domain must be chosen such that wall effect can be removed. Number of particles is considered to be 580,000. Bottom of the body is also placed at an appropriate position which would yield in the intended individual draft based Froude number.

6.1 Comparisons

One of most recent studies for unsteady turbulent simulation of transom flow is the numerical work of Maki et al [8]. Maki [1] had also performed an extensive set of experiments on transom stern flow as a backward facing step. Therefore, Maximum *RMS* of the obtained results is compared with the experiments of Maki [1] conducted on a rectangular hull as well as unsteady turbulent solution of Maki et al [8]. In Maki's [1] experiment, *RMS* of free surface profile at any point *x* was defined as follows:

$$RMS(x) = \left[\frac{1}{N} \sum_{i=1}^{N} (\zeta_i - \bar{\zeta})^2 \right]^{0.5} / T_d \tag{17}$$

in which *N* was number of images (given from a camera) at a fixed location *x*. Accordingly, maximum *RMS* is maximum of the obtained *RMS* at various locations of the free surface profile. Fig. 3 shows a comparison between the current SPH findings, level set results [8] and experimental data [1]. As mentioned earlier, a backward facing step (as a rectangular transom stern) was considered in the experiment by Maki [1]. Figure 3 shows that, in comparison with level set solution, SPH can give more accurate result. Maki et al. [8] used Spalart-Allmaras turbulent model in their simulations. They mentioned that the existing

discrepancies between experimental results and level set findings are due to inaccurate turbulent modeling. This statement seems to be reasonable. Spalart-Allmaras turbulent model is a single equation model for the turbulent viscosity which had been developed for aerodynamic flows [22] while nowadays, LES turbulence model which is also implemented in the current work, has been developed well for large variety of classical free surface flow problems.

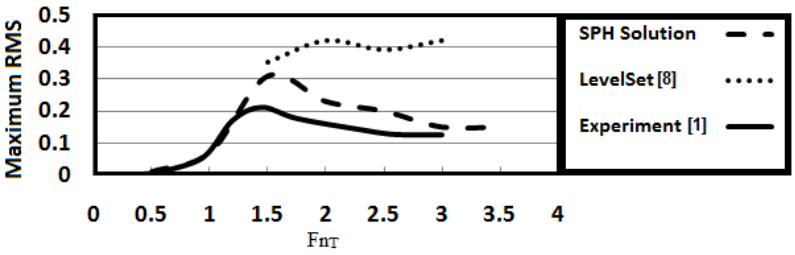

Fig. 3 Maximum RMS (cm) of the free surface profile.

To analyze the obtained values of maximum *RMS* for free surface profile, transition of free surface profile in considered range of draft based Froude numbers are illustrated in Fig. 4. Figs. 4a-d are only depicted at arbitrary instants to qualitatively demonstrate what happens. It is clear that at low draft based Froude numbers (corresponding to Fr_T = 0.5), maximum *RMS* of the free surface profile is very small such that free surface fluctuation may be negligible (Fig. 4a). However, by increasing Fr_T to 1.0, maximum *RMS* increases and when Fr_T is equal to 1.5, maximum *RMS* achieve its highest value. This means that free surface fluctuations are intensified and that some nonlinearity may be expected (Fig. 4b). In the meantime, when Fr_T is increased to 2 and 2.5, maximum *RMS* will be decreased. In this range, ventilation process as well as breaking wave can be captured which are shown in Fig. 4c. Beyond Fr_T = 2.5, variation of free surface profile will be relatively constant and it will be very similar to a regular wave (Fig. 4d). Therefore, free surface profile remains monotonous at various distances from origin of coordinate system (0, 0) (Fig. 2). It must be noted that due to various physical characteristics of transom flow at various Froude numbers, presented data must be depicted at different distance from the origin of coordinate system.

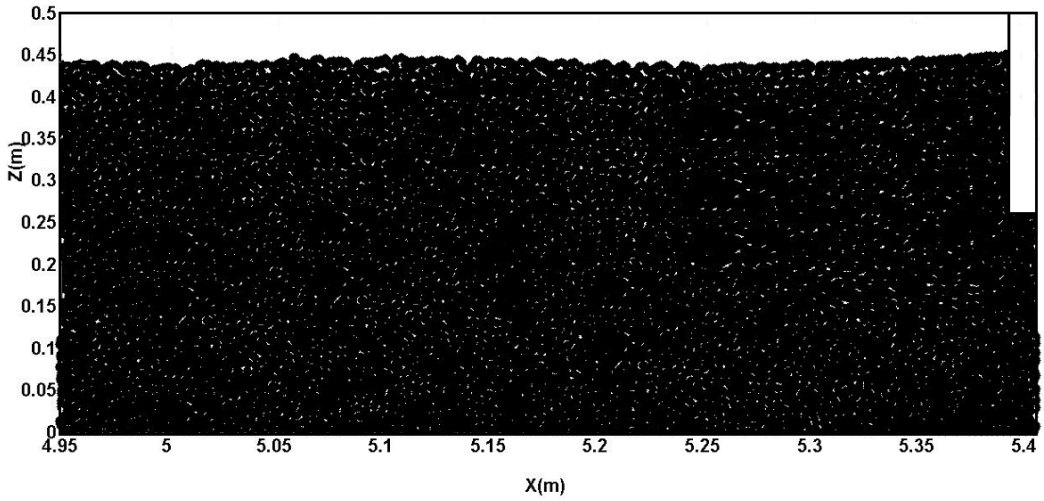

(a) $Fr_T \leq 0.5$

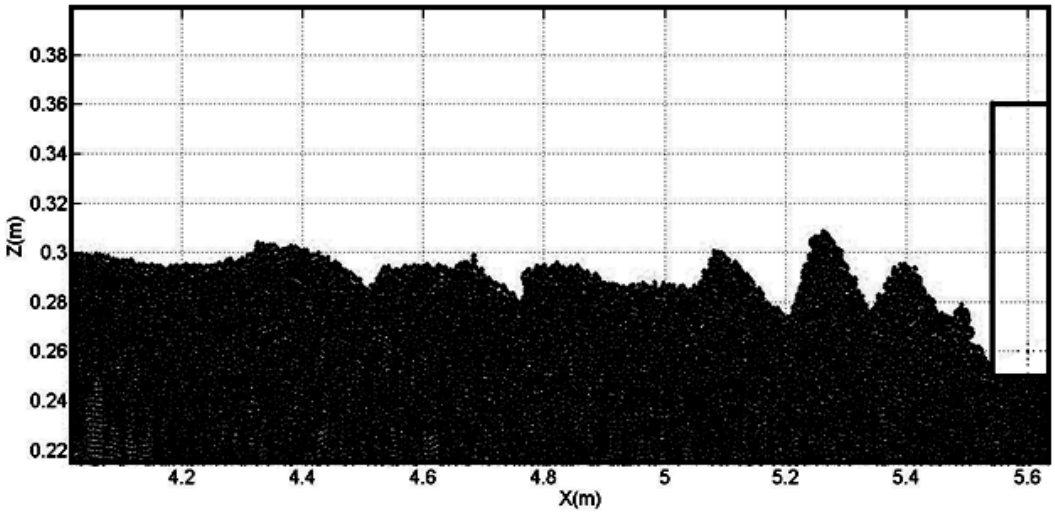

(b) $1.0 < Fr_T \leq 2.0$

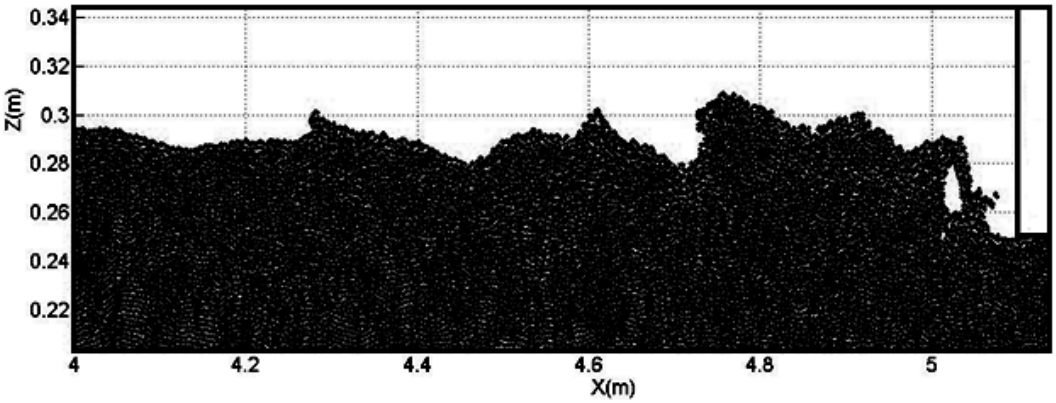

(c) $2.0 < Fr_T \leq 2.5$

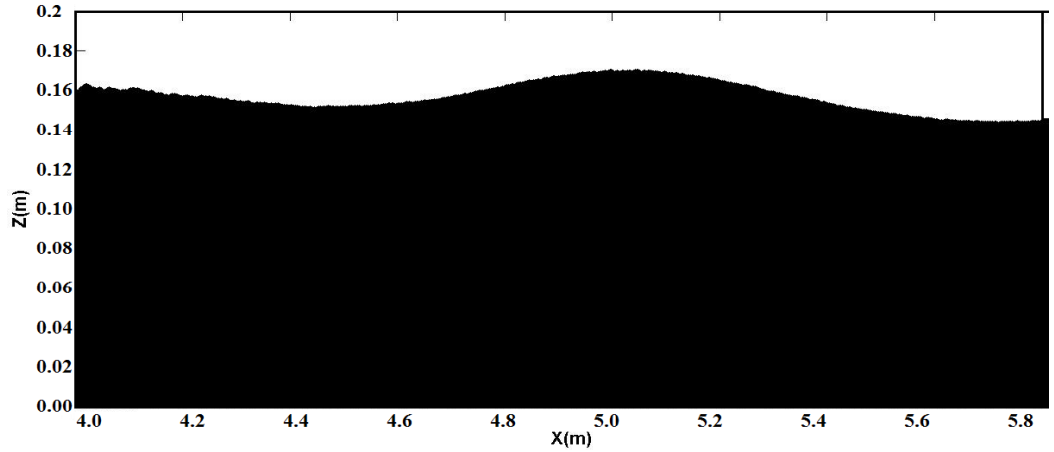

(d) $Fr_T > 2.5$

Fig. 4 Free surface profile at various Fr_T.

For further validation of the presented numerical method, wave slope (S) of the generated wave behind transom stern is also studied. It is worth mentioning that wave slope is a combinatorial effect of wave amplitude and wave length. Therefore, validation of wave slope can lead to validation of wave characteristics. Fig. 5 shows the variation of wave slope on the first wave crest, just behind the transom stern. Maki [8] indicates that the difference between level set and experiment may be due to inaccuracies in the turbulence modeling. In addition to previous descriptions, it must be noted that the Spalart-Allmaras model treated the turbulence in an isotropic way, but near the free surface the turbulence is anisotropic. Anisotropy is the property of being directionally dependent, as opposed to isotropy which implies identical properties in all directions [23]. In the current work, well-known LES turbulence model which has anisotropic properties is implemented. Maki also highlights the omission of surface tension forces in the level set simulations as another reason for this discrepancy.

It is quite evident in Fig. 5 that the SPH method can accurately simulate the transom wave. Moreover, it is observed that various nonlinearities such as ventilation process, large fluctuation and breaking wave occurrence in free surface flow just behind transom can be simulated using SPH method. Therefore, it is expected that the present numerical method can be utilized in the case of high Fr_L, too.

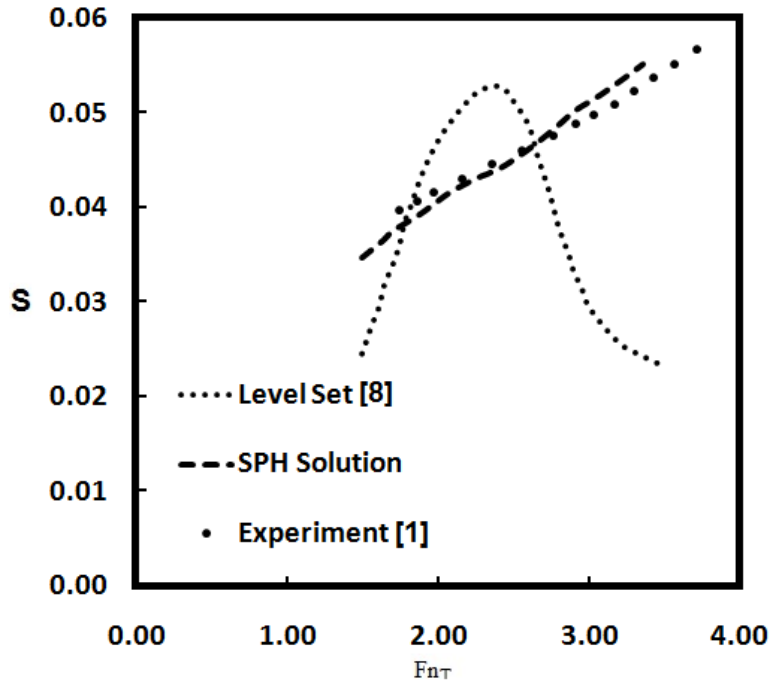

Fig. 5 Comparison of the wave slope against the experimental and numerical data.

7. High speed transom stern flow simulation

In this section, free surface deformation behind high speed body is presented. In the considered simulations, body is moved at three Fr_L with a constant trim angle. However, body is fixed at a constant trim, because it has been shown in the literature that trim angle has no significant effect on the rooster tail behavior [6]. Numerical setup is similar to those of the previous section.

Transom wave generated at Fr_L = 1.0 is illustrated in Fig. 6. It is observed that the wave amplitude is intensified as opposed to the previously considered cases based on the Fr_T. However, high speed transom wave known as rooster tail is invisible, yet. For further

verification of the presented SPH solution, the obtained results are compared with empirical as well as with analytical formulas of Savitsky [4, 6]. These relations were obtained based on various experimental studies and can be good criteria for evaluation of numerical accuracy. Therefore, a comparison presented in Fig.7 shows that the current solution is reasonable. As shown in Figs. 6-12, point zero on the horizontal axis denotes the transom location. Point zero on the vertical axis denotes the bottom of computational domain and wave height is measured from free surface (Z_{FS}) to the lower edge of transom (Z_T). In addition, it is observed that the SPH results are situated in the middle of two Savitsky's formulas. However, it must be noted that Savitsky's formulas are only an approximation for examination of the present results.

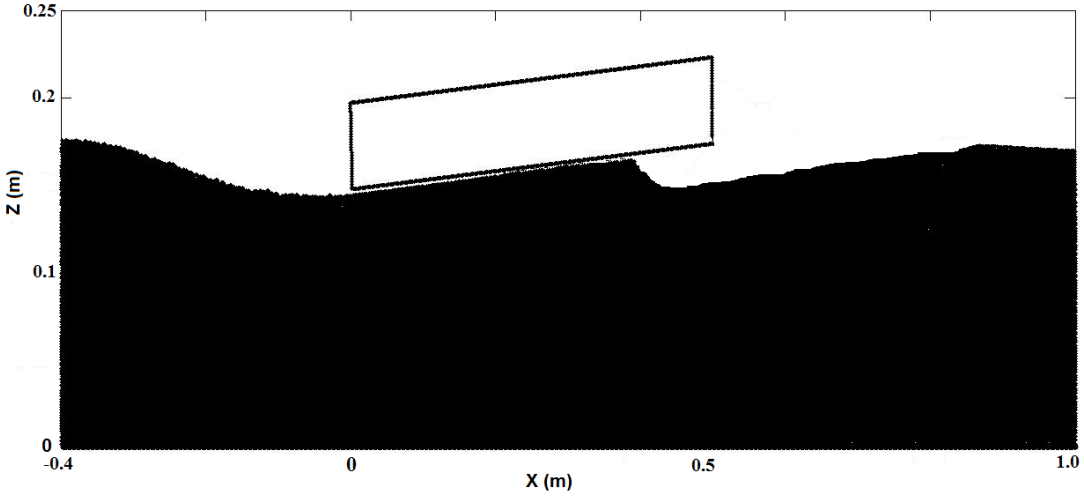

Fig. 6 Free surface profile at Fr_L = 1.0.

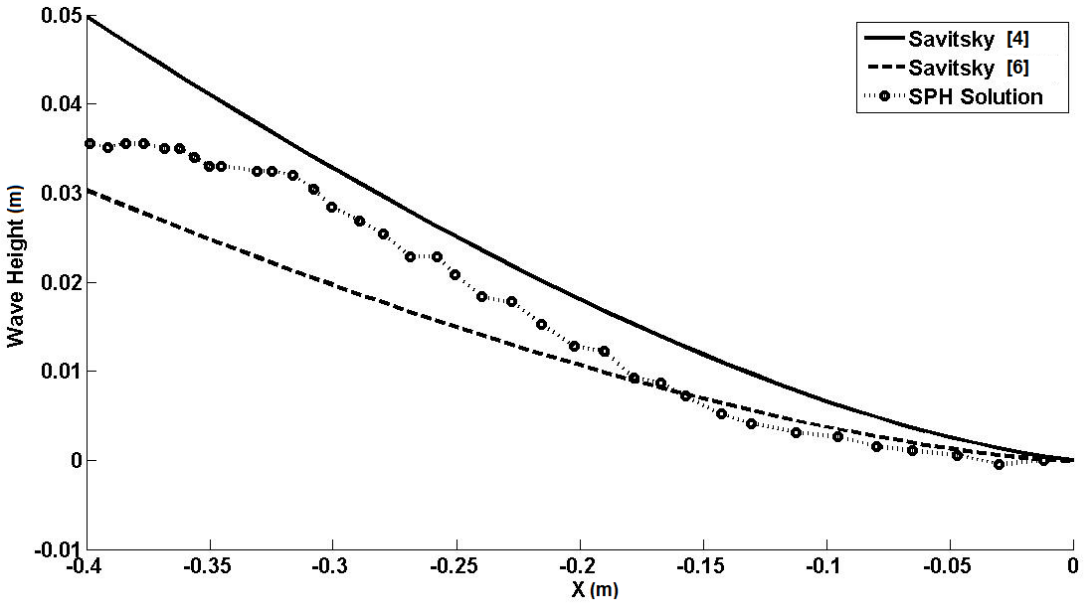

Fig. 7 Comparison of SPH solution with Savitsky's formulas at Fr_L = 1.0.

For more investigations, studies were conducted on transom waves corresponding to two other Froude numbers to examine the effect of Fr_L on the rooster tail formation. Results of transom wave at Fr_L = 1.75 are presented in Fig.8. From Fig.8, it is observed that the wave amplitude is amplified, contrary to the previous case of Fr_L = 1.0. A reduction in the wetted

length of body was also expected. Again, from Fig. 9, it is seen that the SPH solution is located in the middle of Savitsky's formulas.

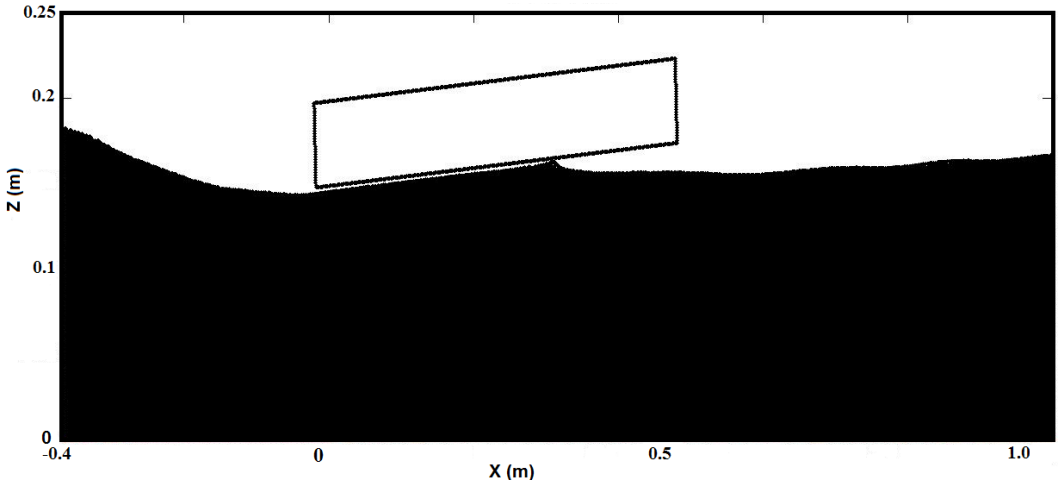

Fig. 8 Free surface profile at Fr_L = 1.75.

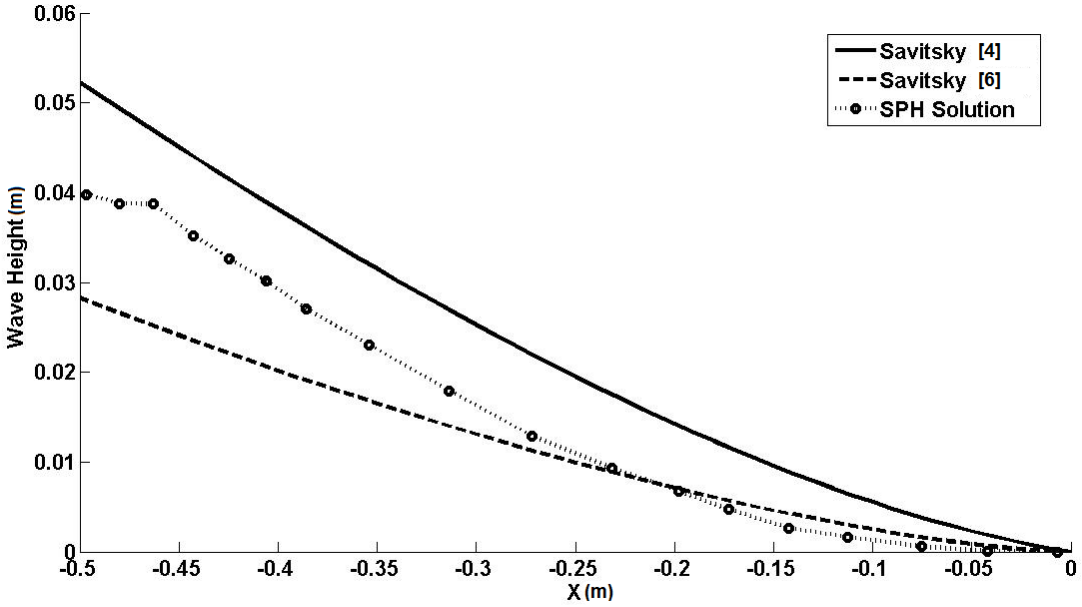

Fig. 9 Comparison of SPH solution with Savitsky's formulas at Fr_L = 1.75.

To accomplish our goal, free surface profile at another Froude number was also surveyed and the Froude number was considered to be 2.85. The obtained solution (Fig. 10) shows that rooster tail is formed, adequately, and wave amplitude is intensified. Wetted length of the body is also decreased. However, in this case, transom wave amplitude is larger than those obtained from Savitsky's formulas, at some locations.

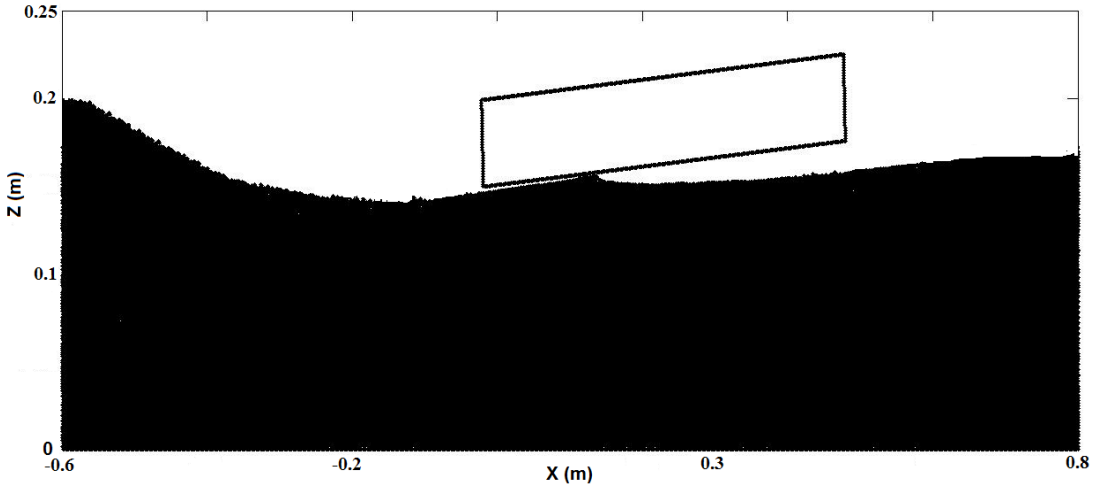

Fig. 10 Free surface profile at Fr_L = 2.85.

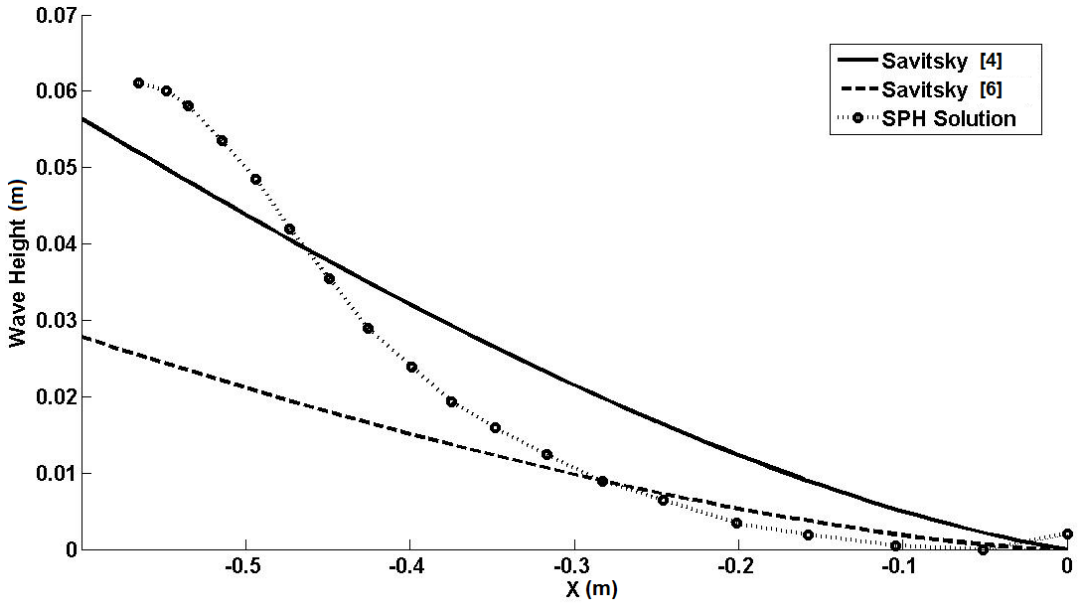

Fig. 11 Comparison of SPH solution with Savitsky's formulas at Fr_L = 2.85.

As stated earlier, in addition to SPH solution of high speed transom wave, another important goal of this study has been to examine the effect of Froude numbers on rooster tail formation. For this purpose, free surface profiles obtained from three earlier solutions are compared with each other. This comparison is displayed in Fig. 12. It is observed that, by increasing Froude number, transom wave is amplified. This can be justified by the fact that when a body moves in a fluid on the free surface, energy is exchanged between the body and the fluid. This energy is radiated from the body in the form of waves. With increased body velocity, more energy is transferred from the body to the fluid. Therefore, by releasing transferred energy, the height of wave behind the transom is amplified and a rigorous wave known as rooster tail is formed. This is completely different from low speed solutions, where challenging the mechanisms of viscosity and wave breaking for diffusing the energy before it, can be radiated by gravity waves. In high speed regime, due to high velocities, there exists no time to diffuse the energy. Moreover, the location of the first wave crest is changed and it is generated at a far distance, relative to the transom location.

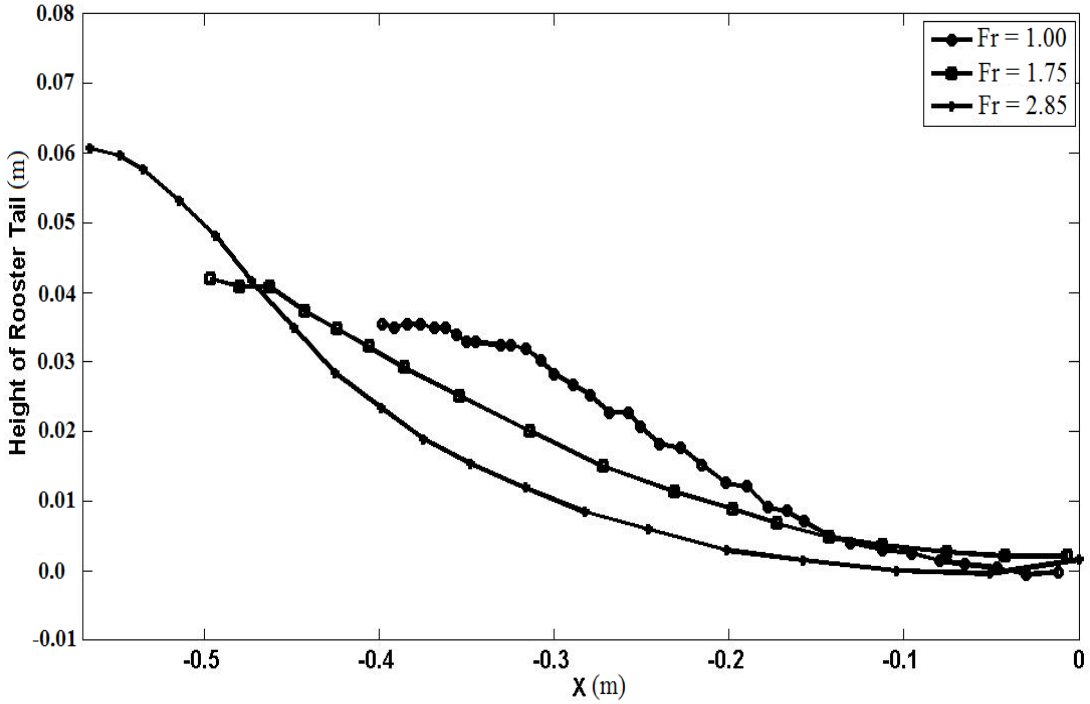

Fig. 12 Effect of Fr_L on the free surface profile.

8. Conclusion

In the present article, high speed transom stern flow simulation is conducted using SPH method. Effort has been made to examine an unsteady turbulent SPH model for more accurate solution of transom stern flow problem at high speed.

Numerical model is considered to be unsteady. SPS turbulent model is employed to improve the numerical results. In addition, a second order density filter is implemented to modify the density field which leads to more accurate simulations. For validation of the current numerical setup, several draft based Froude numbers are considered. A rectangular body is fixed at a desirable draft and body is towed with a constant velocity. The obtained results show that the current SPH setup is quite capable of transom stern simulation. Furthermore, it is observed that various nonlinearities such as ventilation process, large free surface fluctuation, and breaking wave of the problem can be appropriately simulated.

Subsequently, three longitudinal Froude numbers are considered. Free surface profile at the considered Froude numbers is studied and it is found that rooster tail is intensified by increasing the Froude number. Furthermore, the present high speed SPH solutions are compared against Savitsky's formulas and reasonable agreements are achieved.

Study of high speed transom flow at an extensive range of Froude numbers as well as considering propeller effect will be considered as future studies.

REFERENCES

[1] K.J. Maki: *Transom Stern Hydrodynamics*. Doctoral Thesis, University of Michigan, 2006.

[2] L. Doctors, G. Macfarlane, R. Young: *A study on Transom Stern Ventilation*. International Shipbuilding Progress 2007.

[3] J. Doctors: *Hydrodynamic of the Flow Behind a Transom Stern*. Proceeding of the 29th Israel Conference on Mechanical Engineering, Haifa, 2003.

[4] J.K. Maki, J.L. Doctors, R. Beck, A. Troesch: *Transom-Stern Flow for High-Speed Craft*. 8th International Conference on Fast Sea Transportation, Saint Petersburg, Russia, 2005.

[5] D. Savitsky: *Wake Shapes Behind Planing Hull Forms*. Proc. Int. High-Performance Vehicle Conf, pp. VII, Shanghai: The Chinese Society of Naval Architecture and Marine Engineering, pp: 1-15, 1988.

[6] D. Savitsky, M. Morabito: *Surface Wave Contours Associated with the Forebody Wake of Stepped Planing Hulls*. Meeting of the New York Metropolitan Section of the Society of Naval Architects and Marine Engineers, 2009.

[7] H.J. Haussling, R.W. Miller, R.M. Coleman: *Computation of High Speed Turbulent Flow about a Ship Model with a Transom Stern*. Carderock Division, Naval Surface Warfare Center, Hydromechanics Department Report, 1997.

[8] K. Maki, A. Iafrati, S. Rhee, R. Beck, A. Troesch: *The TransomStern Modeled as a Backward Facing Step*. 26th Symposium on Naval Hydrodynamics, Rome, Italy, 2006.

[9] S. Marrone, A. Colagrossi, M. Antuono, C. Lugni, M.P. Tulin: *A 2D+t SPH model to study the breaking wave pattern generated by fast ships*. J. Fluids. Struct **27**, 1199–1215 (2011).

[10] L. Lucy: *A numerical approach to the fission hypothesis*. Astron J., 82-1013 (1977).

[11] R.A. Gingold, J.J. Monaghan: *Smoothed particle hydrodynamics: theory and application to non-spherical stars*. Mon Not Roy Astron Soc, 181-375 (1977).

[12] J.J. Monaghan: *Simulating free surface flows with SPH*. J. Comput. Phys **110**, 399-406 (1994).

[13] J.J. Monaghan: *Smoothed particle hydrodynamics*. Reports on Progress in Physics **68**, 1703–1759 (2005).

[14] P.W. Cleary, M. Prakash, J. Ha, N. Stokes, C. Scott: *Smooth Particle hydrodynamics: status and future potential*. Progress in Computational Fluid Dynamics **7**, 25–76 (2007).

[15] M.B. Liu, G.R. Liu: *Smoothed Particle Hydrodynamics (SPH): an Overview and Recent Developments*. Archives of Computational Methods in Engineering **17**, no: 1, 25-76 (2010).

[16] G.R. Liu, M.B. Liu: *Smoothed Particle Hydrodynamics - a Meshfree Particle Methods*. World Scientific Publ, 2007.

[17] J.J. Monaghan, J.C. Lattanzio: *A refined particle method for astrophysical problems*. Astronomy and *Astrophysics* **149**, 135–143 (1985).

[18] A. Colagrossi, M. Landrini: *Numerical Simulation of Interfacial Flows by Smoothed Particle Hydrodynamics*. J. Comp. Phys. **191**, 448-475 (2003).

[19] A. Crespo: *Application of Smoothed Particle Hydrodynamics Model SPHysics to Free Surface Hydrodynamics*. Doctoral Thesis, 2008.

[20] G.K. Batchelor: *Introduction to Fluid Dynamics*. Cambridge University Press, 1974.

[21] R.A. Dalrymple, B. Rogers: *Numerical Modeling of Water Waves with the SPH Method*. Coastal Engineering **53**, 141-147 (2006).

[22] P.R. Spalart, S.R. Allmaras: *A One-Equation Turbulence Model for Aerodynamic Flows*. AIAA Paper 92-0439, 1992.

[23] C. Georges-Henri, J. Delia, M. Bertrand: *Vorticity dynamics and turbulence models for Large-Eddy Simulations*. ESAIM: Mathematical Modelling and Numerical Analysis **37**, no. 1, 187-207 (2010).

Submitted: 29.10.2012.
Accepted: 06.10.2013.

Abbas Dashtimanesh
Parviz Ghadimi
Dept. Of Marine Technology,
Amirkabir University of Technology, Tehran, Iran